

N94-11385

**ELECTROCHEMICAL CHARACTERIZATION OF  $p^+n$  and  $n^+p$  DIFFUSED InP STRUCTURES**

Maria Faur\*, Mircea Faur, M. Goradia  
Space Photovoltaics Research Center\*\*, Electrical Engineering Department  
Cleveland State University, Cleveland, OH 44115

Carlos Vargas-Aburto  
Kent State University, Kent, OH 44242

David M. Wilt  
NASA Lewis Research Center, Cleveland, OH 44135

The relatively well documented and widely used electrolytes for characterization and processing of Si and GaAs-related materials and structures by electrochemical methods are of little or no use with InP because the electrolytes presently used either dissolve the surface preferentially at the defect areas or form residual oxides and introduce a large density of surface states. Using an electrolyte which we have newly developed for anodic dissolution of InP, and have named the 'FAP' electrolyte, we have performed accurate characterization of InP related structures including nature and density of surface states, defect density and net majority carrier concentration, all as functions of depth. A step-by-step optimization of  $n^+p$  and  $p^+n$  InP structures made by thermal diffusion was done using the electrochemical techniques, and resulted in high performance homojunction InP structures.

**INTRODUCTION**

Electrochemical (EC) techniques represent a simple and yet accurate method to characterize InP and related structures. It is known that using solid-state techniques, a large number of uncertainties in the measurements arise from factors such as gas adsorption, the composition and thickness of front oxide and dead layers, carrier concentration, the quality of contacts, etc.. Using EC techniques these uncertainties can be significantly reduced when both a suitable electrolyte is used and the measuring conditions are properly selected. In addition, EC techniques are of reduced complexity, faster, and allow in-situ recording of a large number of semiconductor characteristics at different depths throughout a structure and in a multilayer structure, within each layer and at the interfaces.

Various surface and bulk semiconductor properties can be determined from electrochemical I-V, C-V and G-V characteristics.

Dark and illuminated I-V characteristics are essential in helping to choose the electrolyte and working conditions for anodic dissolution, surface passivation, revealing of structural defects and EC-V net majority carrier concentration depth profiling. They can also be used in determining various surface and bulk semiconductor properties such as the diffusion length and lifetime of minority carriers and the surface recombination velocity. From illuminated I-V characteristics, the maximum  $J_{sc}$  and  $V_{oc}$  of solar cells fabricated on these structures can be predicted as well.

EC-V characteristics are useful for choosing the electrolyte for which the parasitic components of the total semiconductor/electrolyte interface capacitance, mainly due to residual oxides and surface

\*National Research Council - NASA LeRC Research Associateship

\*\*Funded by NASA Lewis Research Center

states at the interface, are minimal.

Two important parameters for the study of semiconductor materials, namely the flat band potential ( $V_{fb}$ ) and the net majority carrier concentration at a given depth are extracted from the  $1/C^2-V$  characteristics of the semiconductor/electrolyte interface, after dissolution to that depth.

If the electrolyte is well chosen, a very accurate method for determining the density and energy distribution of surface states and traps as a function of depth, applicable to anodic dissolution and surface passivation studies, is based on electrochemical G-V characteristics at low frequencies.

In this work we report on the use of photoelectrochemical techniques for characterization of InP and related material structures. The work focuses on both the characterization and step-by-step optimization of  $n^+p$  and  $p^+n$  InP structures fabricated by thermal diffusion, with application to fabrication of high efficiency, radiation resistant InP solar cells by this method of junction formation. The emitter layer and the junction proximity of the base are characterized as functions of: (a) various surface preparation procedures; (b) diffusion cap; (c) diffusion source, and (d) diffusion conditions (diffusion temperature and time, amount of source material and added phosphorus, and temperature difference between the source and substrates). The EC characteristics of the emitter layer provides: (a) thicknesses of front oxide and damaged layers; (b) density of surface and deep dislocation and precipitates; (c) net majority carrier concentration depth profile, and (d) surface and deep trap level density. The EC characterization was done before and after irradiating the structures with high energy electrons and protons.

In order to maximize the solar cell performances, we also investigated different post-diffusion surface preparation procedures such as removal of the front damaged emitter layer and subsequent surface passivation to obtain smooth, low defect density surfaces with good electrical characteristics.

## EXPERIMENTAL

The experimental study was conducted using a large number of  $n$ ,  $p$ ,  $n^+$  and  $p^+$  InP substrates and thermally diffused  $n^+p$  and  $p^+n$  InP structures. The EC techniques were also tested on epitaxially grown  $n^+p$  and  $p^+nn^+$  InP structures.

We compared our newly developed FAP electrolyte (ref 3) to a selection of previously recommended electrolytes including 0.5M HCl (ref. 1) and the Pear etch (ref 2).

The quality of InP materials and related material structures after anodic dissolution to different depths was characterized by:

- (a) an analysis of dark I-V, illuminated I-V, C-V,  $1/C^2-V$  and G-V characteristics using a commercially available Polaron Profiler (Bio-Rad Polaron PN 4200);
- (b) inspection of surface topography using Nomarski and SEM microscopy;
- (c) Dektak inspection of the craters;
- and, (d) on selected samples, EDAX or XPS study of the surface contaminants and oxidation stage after dissolution in different electrolytes.

In order to optimize the post-diffusion surface preparation procedures and maximize the solar cell performances we investigated the effect of removal of the front damaged emitter layer and surface passivation on liquid-junction electrolyte/InP solar cell parameters.

## RESULTS AND DISCUSSION

Dark and illuminated I-V characteristics were used to study the electrolyte/InP interface with applications ranging from anodic dissolution and surface passivation to predicting the  $J_{sc}$  values of solar cells fabricated on these structures.

From the high values of dark saturation current at the electrolyte/InP liquid junction, using previously recommended electrolytes (i.e., 0.5M HCl and the Pear etch) one can conclude that preferential dissolution of one of the components takes place. Thus, the high dark saturation current densities ( $J_0$ ) are due to the presence of a large surface state density due to such defects as P or In vacancies. An example is given here in the case of 0.5M HCl. We attribute the high  $J_0$  values seen in Figure 1 to surface states introduced by In vacancies as confirmed by XPS and low frequency electrochemical G-V measurements. By comparison, under similar conditions, that is, after the removal of about 300Å from the  $p^+$  InP surface using the FAP electrolyte,  $J_0$  is zero within the measuring capabilities at a reverse bias of up to 1.5V. Also, the illuminated I-V characteristic in this case shows a near ideal behavior. This confirms our XPS and EG-V results which show a near ideal surface stoichiometry and a very low surface state density after dissolving good quality structures using the FAP electrolyte.

From the illuminated electrochemical I-V characteristics of diffused InP structures we were able to predict the maximum short-circuit current density ( $J_{sc}$ ) of solid-state solar cells fabricated on these structures, and to estimate the optimal emitter thickness. We found a very good agreement between the  $J_{sc}$  values of liquid and solid state solar cells. As an example, the maximum  $J_{sc}$  values of a liquid junction  $p^+n$  InP/FAP electrolyte cell was found after dissolving about 0.81µm from the surface (initial emitter thickness ~ 1.15µm). Extrapolating the illumination levels in Figure 2 at 130 mW/cm<sup>2</sup>, the calculated  $J_{sc}$  value is about 33.2 mA/cm<sup>2</sup>. The  $J_{sc}$  value of a solar cell fabricated on a similar structure, prior to AR coating, measured using an ELH lamp at 130mW/cm<sup>2</sup> was 30.7 mA/cm<sup>2</sup>. Since the front contact coverage was about 6.5%, the active area  $J_{sc}$  value becomes 32.8 mA/cm<sup>2</sup>, which within experimental errors is very close to the liquid junction cell  $J_{sc}$  value.

In the case of an optimized thermally diffused  $n^+p$  (S,Zn) InP structure, the effect of removing the highly damaged front  $n^+$  layer on the quality of the emitter is evident in Figure 3 by the variation of the photoelectrochemical  $J_{sc}$  at the FAP electrolyte/ $n^+$  InP liquid junction under a constant low level illumination (~ 5mW/cm<sup>2</sup>) under an incandescent lamp. The  $J_{sc}$  reaches a maximum of about 1.2 mA/cm<sup>2</sup> after removal of about 400Å from the surface, corresponding to surface carrier concentration of about  $2 \times 10^{18}$ cm<sup>-2</sup> (ref 4). Interestingly enough, AES profiling has shown that in this case the phosphorous depleted dead layer also extends to about 400Å below the surface (ref 5). The density of phosphorous vacancy related traps with an energy of 0.24 eV above the valence band calculated from electrochemical G-V plots at 0.8 kHz is shown for this structure in Figure 4 (the lower curve). It reaches a minimum of about  $10^{11}$ cm<sup>-2</sup> eV<sup>-1</sup> also after removing about 400Å from the surface. The  $V_p$ -related hole trap density prior to optimization of the diffusion process was much higher as can be seen in the upper curve. The two structures in this figure were diffused for 3 hours at 660°C using the shown amounts of In<sub>2</sub>S<sub>3</sub> and red phosphorus normalized to the ampoule volume. The optimized structure was diffused through a thin phosphorus rich (~ 50Å thick) diffusion cap layer while the high  $V_p$ -related defect density structure was diffused through a clean surface.

The  $J_{sc}$  value of a solar cell fabricated on the optimized structure, measured using a ELH lamp at 130 mW/cm<sup>2</sup>, was about 31.6 mA/cm<sup>2</sup> (active area, no AR coating) after removing about 400 Å from the surface which is close to the 32.2 mA/cm<sup>2</sup> value calculated by extrapolating the liquid junction cell

$J_{sc}$  value of 1.2 mA/cm<sup>2</sup> mentioned above.

Electrochemical C-V,  $1/C^2$ -V and low frequency G-V characteristics are used not only for characterization of InP materials and structures but also for step-by-step optimization of fabrication procedures of thermally diffused p<sup>+</sup>n and n<sup>+</sup>p InP structures.

As an example, in connection with Figure 5 in the case of our initial p<sup>+</sup>n InP structures a large number of surface and deep defects have been revealed. In this example at the surface of a Cd-doped p<sup>+</sup>n InP (S-doped substrates) we found two trap lines; one of 0.6 eV above the valence band which we believe is a phosphorus vacancy ( $V_p$ ) related defect and another at 0.21 eV below the conduction band which we attributed to interstitial Cd. After removing about 400Å from the surface the deep acceptor-like defect disappeared, but the donor-like defect could still be found in large concentrations, i.e., about  $3 \times 10^{14}$  cm<sup>-2</sup>eV<sup>-1</sup>, maximum value at 0.8 KHz. By using a thin phosphorus-rich (~ 50Å thick) diffusion cap layer and optimized diffusion conditions, the C-V,  $1/C^2$ -V and G-V characteristics recorded at 0.8 KHz at the p<sup>+</sup> InP/FAP electrolyte interface behave normally. The curvatures in  $1/C^2$ -V and G-V characteristics seen in Figure 6a are due to impurities present in the front contamination layer. After removing only about 300Å from the surface, including the front oxide layer (see the decrease in the capacitance), as seen in Figure 6b the three characteristics are quasi-ideal.

The use of FAP electrolyte for EC characterization of diffused and other related InP structures proved to be a very good choice. Although for some applications such as revealing the dislocation density a series of other electrolytes could be used (ref 4), FAP electrolyte is the only good choice we found for mapping the dislocation density (etch pits and precipitates) as a function of depth, which is essential for defect revealing in thin multi-layer InP structures either at a certain depth or at an interface (ref 6).

For other applications such as EC-V profiling, the FAP electrolyte to our knowledge is the only good choice (ref 4). Previously recommended electrolytes such as 0.5M HCl and the Pear etch do not satisfy the criteria of a good electrolyte because of one or more drawbacks such as: dissolving InP preferentially at the defect areas, forming insoluble products on the surfaces, producing rounding at the crater rim, introducing parasitic capacitance components at the electrolyte/InP interface, etc., which result in inaccurate profiles.

Due to its intrinsic qualities (ref 4) the FAP electrolyte appears to be quasi-ideal for performing accurate net majority carrier concentration EC-V profilings. As an example, Figure 7 shows an EC-V profile of an epitaxially grown p<sup>+</sup>nn<sup>+</sup> InP structure. As seen, after profiling the structure to a depth of 6µm, the known n<sup>+</sup> base donor concentration of  $2 \times 10^{18}$  cm<sup>-3</sup> is very close to the recorded value. Additionally, the crater depth measured using a Dektak profilometer, of about 5.85 µm almost coincide with the calculated EC-V depth.

A step-by-step EC characterization of n<sup>+</sup>p (S,Zn), n<sup>+</sup>p (S,Cd), p<sup>+</sup>n (Zn,S) and p<sup>+</sup>n (Cd,S) InP structures, fabricated by thermal diffusion, as a function of processing parameters has helped us not only to improve the fabrication process of diffused structures but also to predict the  $J_{sc}$  and  $V_{oc}$  values of solar cells made from these structures.

For performing such an extensive experimental task EC techniques are much faster and could be more reliable as compared to solid-state techniques. They allow one to study not only the global picture of one of the characteristics of interest as is the case with most of the solid-state techniques but also the variation of these characteristics at different depths throughout the structures.

A significant improvement in the quality of n<sup>+</sup>p and p<sup>+</sup>n InP structures fabricated by closed-ampoule thermal diffusion was obtained after optimizing the diffusion processing using EC techniques for step-by-step characterization of these structures. The investigation was designed to establish: (i) a proper surface preparation procedure prior to diffusion for the substrates; (ii) the right dopant for the

substrates and the right diffusant; (iii) the nature and thickness of the diffusion cap layer; (iv) diffusion temperature and amounts of source materials for doping the substrates below the solubility limit of the doping species; (v) diffusion time for obtaining a desired junction depth; (vi) temperature difference between the substrates and source zones; (vii) thickness of the front dead layer, and (viii) the post-diffusion surface preparation procedure for the removal of the front damaged layer of the surface so as to obtain smooth passivated surfaces with good electrical characteristics.

As an example, a significant reduction of structural defect densities of  $n^+p$  and  $p^+n$  InP structures was obtained after optimizing the diffusion process, as can be seen in Tables 1 and 2 (ref 6). For  $n^+p$  structures, the lowest etch pit density (EPD) of  $6 \times 10^5 \text{ cm}^{-2}$  was achieved after S diffusion into InP:Cd ( $N_A \sim 1.2 \times 10^{16} \text{ cm}^{-3}$ ) substrates using a thin  $\text{In}(\text{PO}_3)_3$ -rich anodic oxide diffusion cap layer at a diffusion temperature of  $660^\circ\text{C}$ , while the lowest EPD after S diffusion into InP:Zn ( $N_A \sim 2 \times 10^{16} \text{ cm}^{-3}$ ) under similar diffusion conditions was  $8 \times 10^6 \text{ cm}^{-2}$ . For  $p^+n$  structures, surface EPD values as low as  $2 \times 10^2 \text{ cm}^{-2}$  were achieved in the case of Cd diffusion into InP:S ( $N_D = 3.5 \times 10^{16} \text{ cm}^{-3}$ ) substrates at a diffusion temperature of  $560^\circ\text{C}$  using a thin  $\text{In}(\text{PO}_3)_3$ -rich chemical oxide diffusion cap layer, while the lowest EPD in the case of Zn diffusion was  $3 \times 10^5 \text{ cm}^{-2}$ . The differences are explained by the large number of  $\text{In}_2\text{S}_3$ , InS and  $\text{Zn}_3\text{P}_2$  surface and deep precipitates detected in the case of  $n^+p$  (S,Zn) and  $p^+n$  (Zn,S) InP structures.

From the EC characteristics for our diffused structures, we found the ranking in decreasing order of projected maximum efficiency to be: (1)  $p^+n$  (Cd,S), (2)  $n^+p$  (S,Cd), (3)  $p^+n$  (Zn,S), (4)  $n^+p$  (S,Zn). The AMO,  $25^\circ\text{C}$  efficiency of solar cells fabricated on these structures have confirmed that the maximum efficiency could be obtained in the case of  $p^+n$  (Cd,S) solar cells while the worst performances were recorded in the case of  $n^+p$  (S,Zn) cells. A preliminary EC investigation of  $p^+n$  (Cd,S),  $n^+p$  (S,Cd) and  $p^+n$  (Zn,S) structures both prior to and after irradiation with  $10^{13} \text{ cm}^{-2}$  of 3 MeV protons, which includes studies of electrical and structural defect densities and net majority carrier concentration variations in the emitter and the immediate junction proximity of the base, seems to indicate that the same ranking as above holds for radiation tolerance. Therefore, we have lately concentrated our efforts on optimizing the  $p^+n$  InP (Cd,S) diffused structures so as to achieve high-efficiency, radiation resistant InP solar cells by this method of junction formation. As a result, the maximum AMO,  $25^\circ\text{C}$  open circuit voltage ( $V_{oc}$ ) values of bare solar cells have reached 880 mV which as far as we know is the highest value reported to date for any InP solar cell (ref 7).

## CONCLUSIONS

As a process control tool, EC techniques are faster and of reduced complexity compared to solid-state techniques. In addition, the use of EC techniques allows in-situ recording of a large number of semiconductor characteristics at different depths throughout the structure and, in a multilayer structure, within each layer and at the interfaces.

It is our opinion that EC techniques are or could become more accurate than any known solid-state techniques for performing majority and possibly minority doping concentration depth profilings, as well as for the mapping of structural and electrical type defect densities as functions of depth.

Using improved EC characterization techniques for step-by-step optimization of  $n^+p$  and  $p^+n$  InP diffused structures has made it possible to fabricate high performance homojunction InP structures.

## REFERENCES

- [1]. T. Ambridge and D. J. Ashen, *Electron Lett.* 15, 674 (1979).
- [2]. R. T. Green, D. K. Walker and C. M. Wolfe, *J. Electrochem. Soc.* 133(11), 2278 (1986).
- [3]. Maria Faur, Mircea Faur, Patent pending (1992).
- [4]. Maria Faur, Mircea Faur, I. Weinberg, M. Goradia, and C. Vargas, *Proceedings of the 11th SPRAT Conference*, May 7-9, 1991, p. 7-1.
- [5]. Mircea Faur, Maria Faur, F. Honey, C. Goradia, M. Goradia, D. Jayne and R. Clark, *J. Vac. Sci. Technol. B10* (4), 1277 (1992).
- [6]. Mircea Faur, Maria Faur, C. Goradia, M. Goradia, and I. Weinberg, *Proceedings of the 4th Int. Conf. on InP and Related Materials*, Newport, Rhode Island, April 20-24, 1992, p. 322.
- [7]. Mircea Faur, Maria Faur, C. Goradia, M. Goradia, D. J. Flood, D. J. Brinker, I. Weinberg, C. Vargas, and N. S. Fatemi, this Conference.

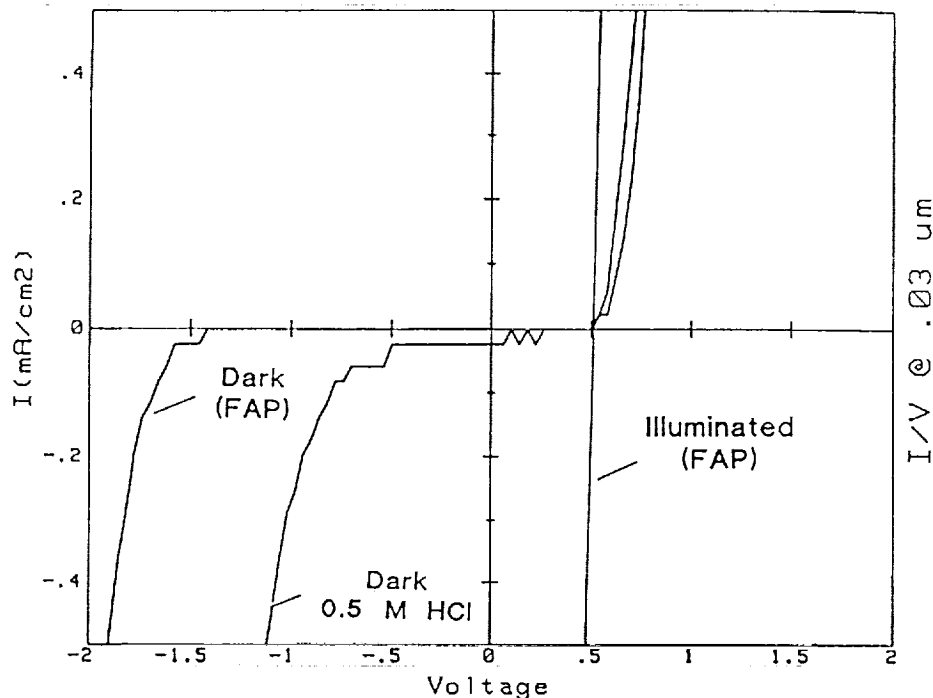


Figure 1. I-V characteristics of  $p^+n$  InP/electrolyte after removing  $0.03 \mu\text{m}$  from the surface using  $0.5\text{M HCl}$  and the FAP electrolytes.

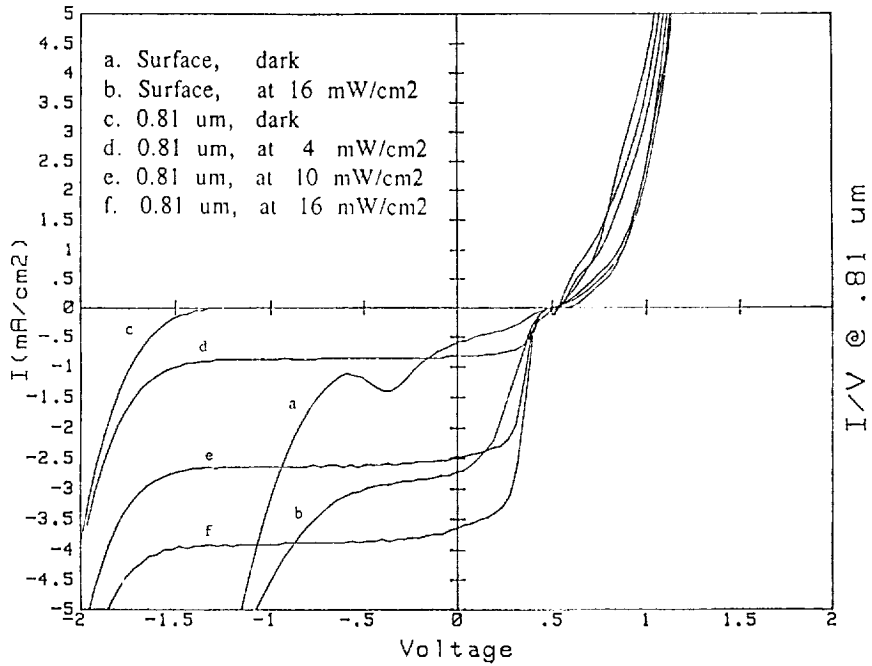


Figure 2. Dark and illuminated I-V characteristics of p+n(Cd,S) InP/FAP electrolyte junction prior to and after the removal of 0.81  $\mu\text{m}$  from the surface.

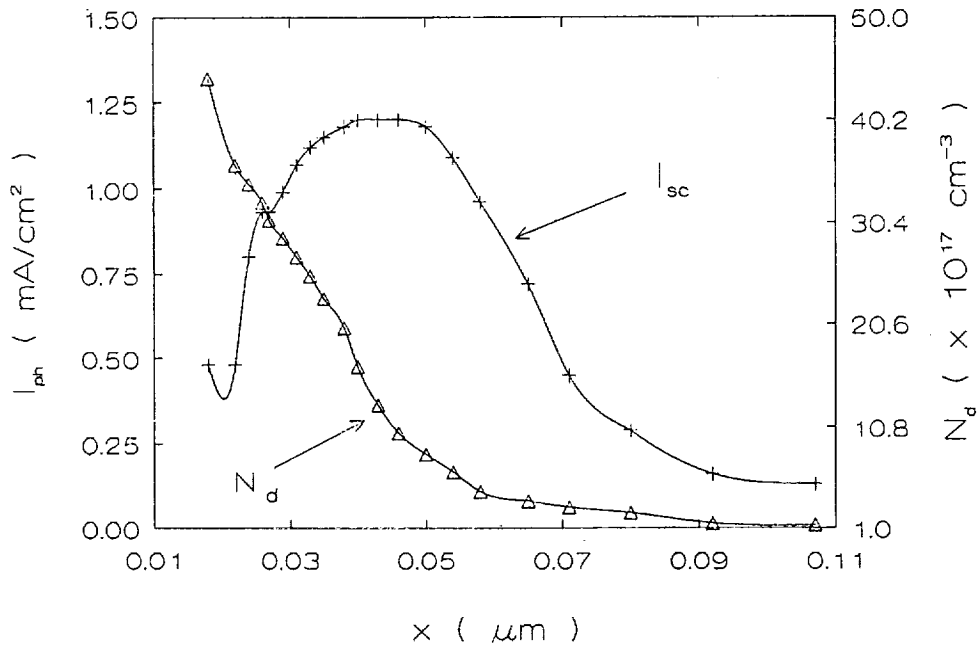


Figure 3. Variation of  $J_{sc}$  and net majority carrier concentration ( $N_D$ ) as a function of dissolution depth of an optimized n+p(S,Zn) InP structure. Diffusion temperature: 600°C; Diffusion time: 3 hours. Normalized amounts of source and red P: 200  $\mu\text{g}$   $\text{In}_2\text{S}_3/\text{cm}^3$  and 75  $\mu\text{g}$   $\text{P}/\text{cm}^3$ .

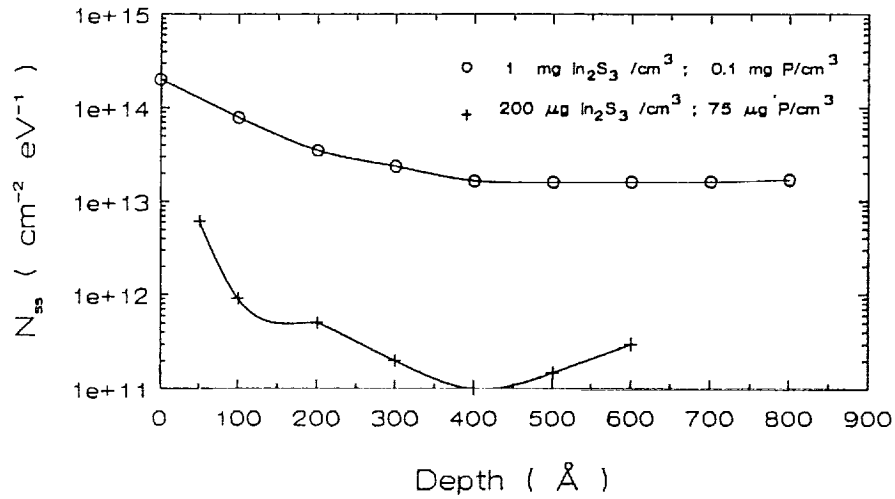


Figure 4. Surface state density ( $N_{ss}$ ) after anodic dissolution of n<sup>+</sup>p InP structures made by S-diffusion into Zn-doped ( $N_A = 8 \times 10^{15} \text{ cm}^{-3}$ ) substrates. Diffusion temperature: 660°C; Diffusion time: 3 hours.

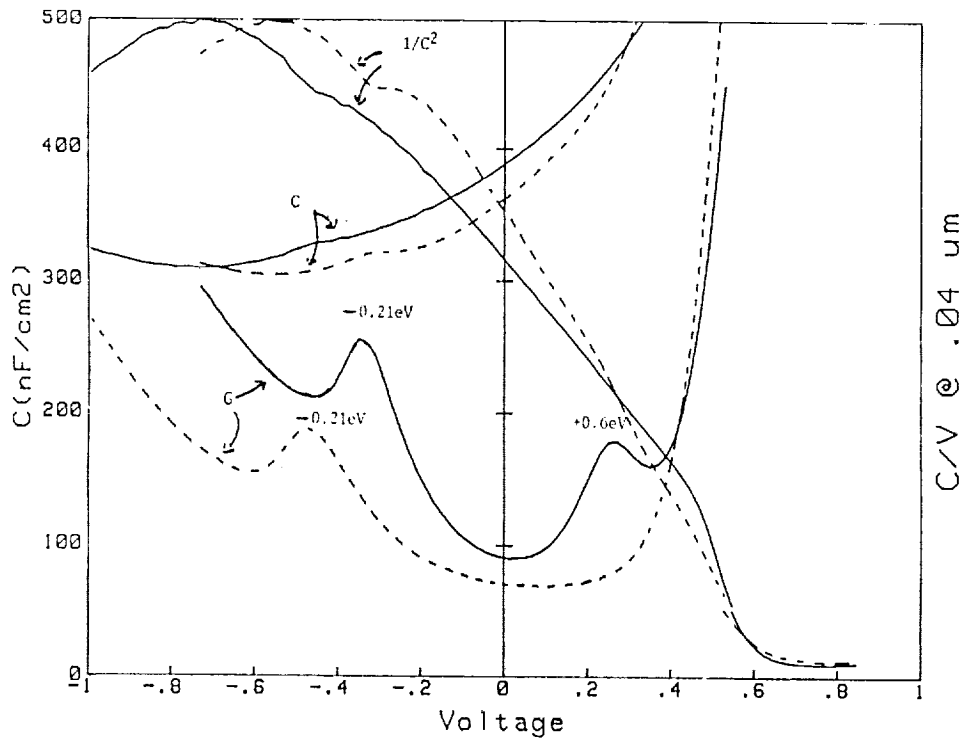


Figure 5. Electrochemical C-V, G-V, and  $1/C^2$ -V plots before (solid line) and after (dashed line) removal of  $0.04 \mu\text{m}$  from the surface of a p<sup>+</sup>n(Cd,S) InP thermally diffused structure.



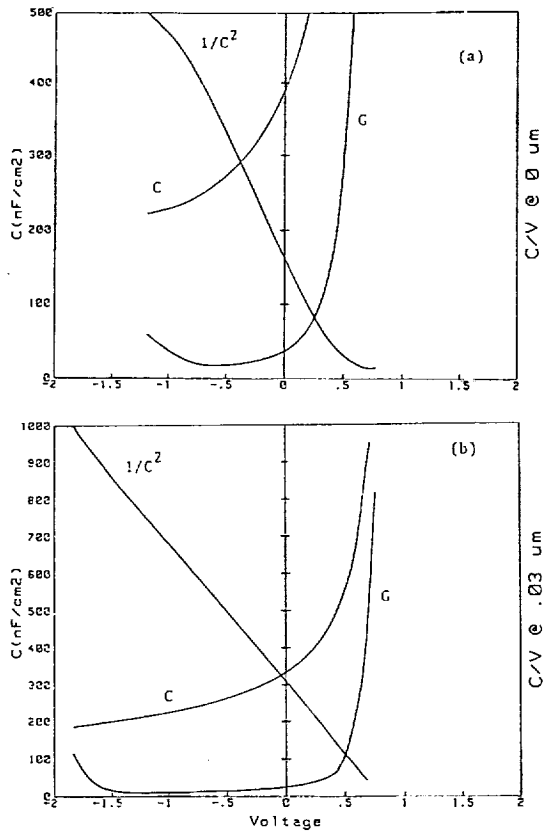


Figure 6. Electrochemical C-V, G-V, and  $1/C^2$ -V plots: (a) prior to and after removing  $0.03 \mu\text{m}$  from the surface of an optimized  $\text{p}^+\text{n}(\text{Cd,S}) \text{InP}$  structure.

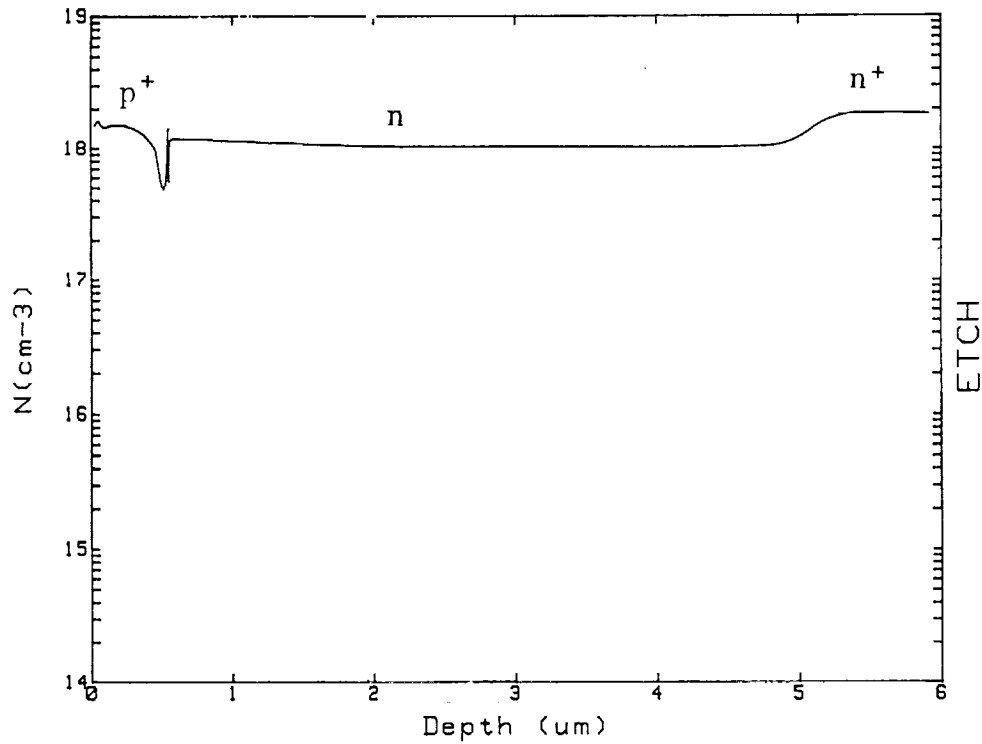


Figure 7. EC-V net carrier concentration depth profile of an epitaxially grown  $\text{p}^+\text{nn}^+$  InP structure.

**Table 1.** Surface EPD and precipitates of  $n^+p$  InP structures diffused at  $660^\circ\text{C}$  through bare and capped surfaces.

Structure	Diffusion Cap	Surface EPD ( $\text{cm}^{-2}$ )	Surface Precipitates	Deep
$n^+p$ (S,Zn)	Bare	$6 \times 10^8$	$\text{In}_2\text{S}_3$	ZnS
$n^+p$ (S,Cd)	Surface	$3 \times 10^7$	$\text{In}_2\text{S}_3$	--
$n^+p$ (S,Zn)	$\text{In}(\text{PO}_3)_3$	$8 \times 10^6$	$\text{In}_2\text{S}_3$	--
$n^+p$ (S,Cd)	( $\approx 50\text{\AA}$ )	$6 \times 10^5$	$\text{In}_2\text{S}_3$	--

**Table 2.** Surface EPD and precipitates in  $p^+n$  InP structures.

Structure	Diffusion Cap	Diffusion Temp ( $^\circ\text{C}$ )	Surface EPD ( $\text{cm}^{-2}$ )	Surface Precipitates	Deep
$p^+n$ (Zn,S)	Bare	520	$5 \times 10^7$	$\text{Zn}_3\text{P}_2$	$\text{Zn}_3\text{P}_2$
$p^+n$ (Cd,S)	Surface	560	$7 \times 10^5$	$\text{Cd}_3\text{P}_2$	--
$p^+n$ (Zn,S)	$\text{In}(\text{PO}_3)_3$	520	$3 \times 10^5$	$\text{Zn}_3\text{P}_2$	$\text{Zn}_3\text{P}_2$
$p^+n$ (Cd,S)	( $\approx 40\text{\AA}$ )	560	$2 \times 10^2$	--	--